ISSN 0915-633X

NIFS--392
JP9604038

NATIONAL INSTITUTE FOR FUSION SCIENCE

Self-organization Process of a Magnetohydrodynamic Plasma in the Presence of Thermal Conduction

Shao-ping Zhu, R. Horiuchi, T. Sato
and The Complexity Simulation Group

(Received - Dec. 1, 1995)

NIFS-392 Dec. 1995

RESEARCH REPORT
NIFS Series

VOL 27 № 15

NAGOYA, JAPAN

This report was prepared as a preprint of work performed as a collaboration research of the National Institute for Fusion Science (NIFS) of Japan. This document is intended for information only and for future publication in a journal after some rearrangements of its contents.

Inquiries about copyright and reproduction should be addressed to the Research Information Center, National Institute for Fusion Science, Nagoya 464-01, Japan.

SELF-ORGANIZATION PROCESS OF A MAGNETOHYDRODYNAMIC PLASMA IN THE PRESENCE OF THERMAL CONDUCTION

Shao-ping Zhu[1], Ritoku Horiuchi,[1,2] and Tetsuya Sato[1,2]
and
The Complexity Simulation Group[2,†]

[1] Department of Fusion Science, The Graduate University for Advanced Studies, Nagoya 464-01, Japan

[2] Theory and Computer Simulation Center, National Institute for Fusion Science, Nagoya 464-01, Japan

Abstract

A self-organization process of a magnetohydrodynamic(MHD) plasma with a finite thermal conductivity is investigated by means of a three-dimensional MHD simulation. With no thermal conduction an MHD system self-organizes to a non-Taylor's state in which the electric current perpendicular to the magnetic field remains comparable to the parallel electric current. In the presence of thermal conductivity the perpendicular component of electric current and the nonuniformity of thermal pressure generated by driven reconnection tend to be smoothened. Thus, the self-organized state approaches to a force-free minimum energy state under the influence of thermal conduction. Detailed energy conversion processes are also studied to find that the rapid decay of magnetic energy during the self-organization process is caused not only through the ohmic heating, but also through the work done by the $\mathbf{j} \times \mathbf{B}$ force.

Keywords: magnetohydrodynamic simulation, work done by magnetic force, ohmic heating, thermal conduction, self-organization

---

†K.Watanabe, T.Hayashi, Y.Todo, T.H.Watanabe, A.Kageyama and H.Takamaru

In our recent paper[1], it is disclosed that the Taylor's force-free minimum energy state[2-4] is only approximately realized in energy relaxation process of a magnetohydrodynamic (MHD) plasma. In general, an MHD plasma relaxes towards a force-balanced minimum energy state where the thermal energy (pressure) distribution exhibits a structure similar to the Taylor's magnetic structure. The process is as follows. The driven magnetic reconnection process produces an extremely heated plasma in the vicinity of a reconnection point. The locally heated plasma modifies the magnetic field through the pressure gradient force. Consequently, the perpendicular electric current is generated so as to balance with the pressure gradient force. The new self-organized state of a finite pressure MHD plasma is an MHD equilibrium $\mathbf{j} \times \mathbf{B} = \nabla p$, instead of the Taylor's force-free minimum energy state.

The thermal conduction, especially perpendicular to the magnetic field, smoothes out the peaked pressure profile produced by driven magnetic reconnection. Therefore, the self-organized state is expected to approach to a force-free profile in accordance with increase of thermal conductivity. In the present paper, we carry out a three-dimensional simulation for a resistive MHD plasma with a finite thermal conductivity but with no viscosity and clarify the effect of thermal conduction on the self-organization process by comparing with the simulation results for a zero thermal conductivity case. We also touch on the details of the energy conversion processes in the self-organization process.

The simulation model is the same as the one used in the previous paper[1], expect for addition of a thermal conduction term for the pressure equation, i.e., $\kappa \nabla^2 p$. The initial condition and the boundary condition are also the same as the previous case ($L_t/L_p = 5$)[1, 5].

Three simulation runs with different thermal conductivities are carried out. The simulation parameters are listed in Table 1. In the following discussion, we examine the simulation result for Case A in Table 1 unless otherwise stated.

In our previous paper[1], two important characteristics of the self-organization of an MHD plasma have been clarified by a three-dimensional MHD simulation study, namely, (1) selective decay of magnetic energy, and (2) critical slowing-down of the dissipation of magnetic helicity. Figure 1 shows the temporal evolutions of the total magnetic energy W, the total magnetic helicity K and their ratio W/K, where W and K are normalized by their initial values and the time is normalized by the Alfven transit time t_A. The behavior of the ratio W/K illustrates that there exist two relaxation phases in the temporal evolution, i.e., the first relaxation phase ($18t_A < t < 25t_A$) and the second relaxation phase ($36t_A < t < 44t_A$). The magnetic energy decays rapidly in the relaxation phases in the time scale comparable to the Alfven transit time. In contrast to the stepwise relaxation of magnetic energy, the magnetic helicity exhibits explicitly the stepwise slowing-down in the dissipation rate in accordance with the stepwise drop of magnetic energy.

As we have already explained in the previous paper[1], the critical slowing-down of the dissipation of magnetic helicity is due to the formation of a negatively peaked profile of $\mathbf{j} \cdot \mathbf{B}$ at a reconnection point as a result of driven magnetic reconnection. (Note that the relation $\mathbf{j} \cdot \mathbf{B} > 0$ holds everywhere in the initial profile.) On the other hand, the peaked reconnection current causes rapid decay of magnetic energy. Figure 2 shows the temporal evolutions of the total energy decay $D_{MW} + D_{OH}$ and the helicity dissipation D_K, where $D_{MW} = \int \mathbf{v} \cdot (\mathbf{j} \times \mathbf{B}) d^3\mathbf{x}$, $D_{OH} = \eta \int \mathbf{j} \cdot \mathbf{j} d^3\mathbf{x}$ and $D_K = \eta \int (\mathbf{j} \cdot \mathbf{B}) d^3\mathbf{x}$. The rapid increase of $D_{MW} + D_{OH}$ and the stepwise decrease of D_K are obviously explainable of the stepwise decrease of magnetic energy and the slowing-down of magnetic helicity decay rate.

We shall now investigate the detailed processes of the conversion rates of magnetic energy. Fig.3 shows the temporal changes of D_{OH} and D_{MW}. In the initial phase ($0 < t < 18t_A$), D_{OH} decreases linealy, but D_{MW} is negligibly small because the helical kink mode is much smaller than the initial equilibrium field and hence the force-free relation approximately holds. However, The energy conversion rates, D_{OH} and D_{MW},

increase drastically as soon as the first and second relaxations set in. These drastic phenomena correspond to the rapid decays of magnetic energy in the first and second relaxation phases(see Fig.1). It is worthy to note in Fig.3 that the work done by magnetic force becomes comparable to the ohmic heating in the first relaxation phase. Interestingly, it is observed that the backward conversion from the kinetic energy to the magnetic energy takes place in the subsequent phase of the fast decay($D_{MW} < 0$), i.e., the dynamo action. These observations indicate that the rapid decay of magnetic energy in the relaxation phases is a combination of the fast ohmic heating and the work done by the magnetic force $\mathbf{j} \times \mathbf{B}$. In Fig.3 we also plot the conversion rate from the kinetic to thermal energy D_{TW}, where $D_{TW} = \int \mathbf{v} \cdot \nabla p d^3\mathbf{x}$. It is seen that this conversion is not so dominant as D_{MW} and D_{OH}.

Then, we shall investigate the effect of thermal conductivity on the self-organization process. It is likely that a self-organized state approaches to a Taylor's force-free state in the presence of a large thermal conductivity, because the thermal conductivity acts to remove the pressure nonuniformity. Figure 4 shows the temporal evolutions of the total magnetic energy and helicity for three different thermal conductivities, namely, for Cases A, B and C (see Table 1). The onset time of magnetic reconnection becomes shorter as the thermal conductivity increases. This is because thermal conductivity acts to smoothen the pressure profile and break the balance between the thermal and magnetic forces, thus the growth of the helical kink mode is quickened.

Figure 5 shows the temporal evolutions of the nonunifomity index of the pressure distribution, which is defined by

$$\delta p = \left\{ \frac{< (p - < p >)^2 >}{< p >^2} \right\}^{1/2} \tag{1}$$

for the cases of three different thermal conductivities, where $< f(\mathbf{x}) >$ stands for the average of $f(\mathbf{x})$ over the whole volume. The pressure nonuniformity δp in the initial phase becomes smaller as the thermal conductivity increases. As soon as the first relaxation

ence of thermal conduction by means of a three-dimensional simulation. For the case of zero thermal conductivity, the system relaxes to a self-organized state in which the diamagnetic component remains comparable to the force-free component in the electric current. It is found that the diamagnetic component or equivalently the pressure gradient disappears gradually in accordance with the increase of thermal conductivity, namely, the self-organized state of an MHD plasma approches to a Taylor's force-free state under the influence of thermal conduction.

It is also found that the role of kinetic energy is important in considering the dynamical process of self-organization, although it is much smaller than the magnetic and thermal energy. The plasma flow created by the helical kink instability modifes the equilibrium profile and leads to the formation of peaked reconnection current. The enhanced reconnection current plays an important role in the rapid conversion of magnetic energy through two physical processes. The first one is the conversion process of magnetic energy to thermal energy through the enhanced ohmic heating and the second is the conversion process of magnetic energy to kinetic energy through the work done by the magnetic force, namely, plasma acceleration. The present study has demonstrated that the energy conversion through the work done by the magnetic force is imporatant to explain the fast decay of magnetic energy. It is observed that the kinetic energy generated in the relaxation phase is partly returned to magnetic energy(dynamo process) and partly converted into thermal energy by compressional heating. Thus, the kinetic energy decreases to a negligibly low level at the self-organized state.

In the present study we have ignored the effect of viscosity. This process is under investigation.

sets in, δp suddenly increases. The peak value of the pressure nonuniformity is inversely proportional to the thermal conductivity. The system relaxes into a self-organized state after the second relaxation phase. The pressure nonuniformity at the self-organized state remains finite but its value becomes smaller as the thermal conductivity increases. The beta value of the nonuniformity of the thermal pressure $\Delta\beta$ at the self-organized state is listed in Table 2, where $\Delta\beta$ is defined by $\Delta\beta = 2\sqrt{< (p- < p >)^2 >}/ < \mathbf{B}^2 >$. It is clear in Table 2 that the beta value of the pressure nonuniformity disappears gradually as the thermal conductivity increases. It should be noted that a visible spatial structure of the thermal pressure, shown in Fig.6, remains at the self-organized state even for a large thermal conductivity case, although the nonuniformity of thermal pressure is much smaller than the magnetic pressure($\Delta\beta = 0.057 \ll 1$). It should be noted that the structure of thermal pressure is very similar to that of magnetic field.

According to the self-organization theory of pressureless plasma, the self-organized state is force-free. This implies that the perpendicular electric current vanishes at the self-organized state. We plot the temporal evolutions of the force-free (parallel) and diamagnetic (perpendicular) currents in Fig.7 for three different thermal conductivities, where $J_{\|} =< |\mathbf{j}_{\|}|/|\mathbf{j}| >$, $J_{\perp} =< |\mathbf{j}_{\perp}|/|\mathbf{j}| >$, $\mathbf{j}_{\|} = (\mathbf{j}\cdot\mathbf{B})\mathbf{B}/(\mathbf{B}\cdot\mathbf{B})$, and $\mathbf{j}_{\perp} = \mathbf{j} - \mathbf{j}_{\|}$. From this figure one can evidently see that the perpendicular component increases rapidly in accordance with the growth of the ideal kink instability in the first relaxation phase. It increases again in the second relaxation phase and reaches a maximum value. We can see from Fig.7 that the perpendicular electric current at self-organized state is comparable to the parallel component for the zero thermal conductivity case (Case A) and it decreases as the thermal conductivity increases. These results lead us to the conclusion that the system relaxes to a self-organization state close to a Taylor's force-free state in the presence of large thermal conductivity.

We have investigated the self-organization process of an MHD plasma in the pres-

References

[1] S. P. Zhu, R. Horiuchi, T. Sato and The Complexity Simulation Group, Phys.Rev.E, **51**, 6047(1995).

[2] J. B. Taylor, Phys. Rev. Lett. **33**, 1139(1974)

[3] J. B. Taylor, Rev. Mod. Phys. **58**, 741(1986),and references therein.

[4] A. Reiman, Phys. Fluids **23**, 230(1980).

[5] R. Horiuchi and T. Sato, Phys. Rev. Lett.**55**, 211(1985); R. Horiuchi and T. Sato, Phys. Fluids **29**, 1161, 4174(1986); **33**, 1142(1988).

Table 1. Simulation parameters

Case	α	$\frac{L_t}{L_p}$	β	η	κ
A	58.3	5	0.6	2×10^{-4}	0.0
B	58.3	5	0.6	2×10^{-4}	10^{-3}
C	58.3	5	0.6	2×10^{-4}	5×10^{-3}

Table 2. Beta values at self-organized state

Case	κ	$\Delta\beta$
A	0.0	0.12
B	10^{-3}	0.08
C	5×10^{-3}	0.057

Figure Captions

Figure.1 Temporal evolutions of the total magnetic energy W (dot-dashed line), the total magnetic helicity K (solid line) and W/K(dotted line) for case A, where both the energy and the helicity are normalized by their initial values.

Figure.2 Temporal evolutions of the energy decay, $D_{MW} + D_{OH}$(solid line) and the helicity dissipation, D_K(dot-dashed line) for case A, where both $D_{MW} + D_{OH}$ and D_K are normalized by their initial values.

Figure.3 Temporal evolutions of the ohmic heating D_{OH} (solid line), the work done by magnetic force D_{MW} (dashed line) and the work done by thermal force D_{TW} (dot-dashed line) for the same case as Fig.1.

Figure.4 Temporal evolutions of magnetic energy and helicity for Cases A (solid line), Case B (dotted line) and Case C (dot-dashed line).

Figure.5 Temporal evolutions of the pressure nonuniformity δp for the same cases as Fig.5.

Figure.6 A three-dimensional display of the isosurfaces of the toroidal magnetic field and the pressure at $t = 70.55 t_A$ for Case C.

Figure.7 Temporal envolutions of the normalized parallel component $J_{\|}$ and the normalized perpendicular component $J_{\perp}$ of the electric current for the same cases as Fig.5, where $J_{\|} =< |j_{\|}|/|j| >$ and $J_{\perp} =< |j_{\perp}|/|j| >$.

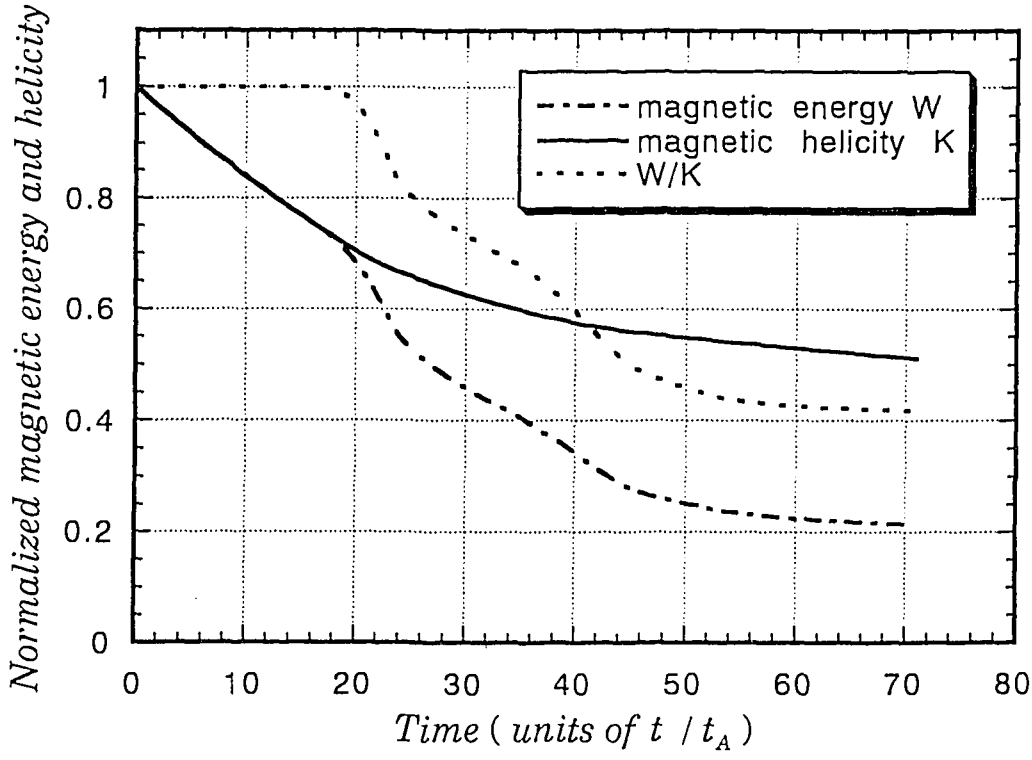
Normalized magnetic energy and helicity
magnetic energy W
magnetic helicity K
W/K
0
0.2
0.4
0.6
0.8
1
0
10
20
30
40
50
60
70
80
Time (units of t / t_A)

*Fig.*1

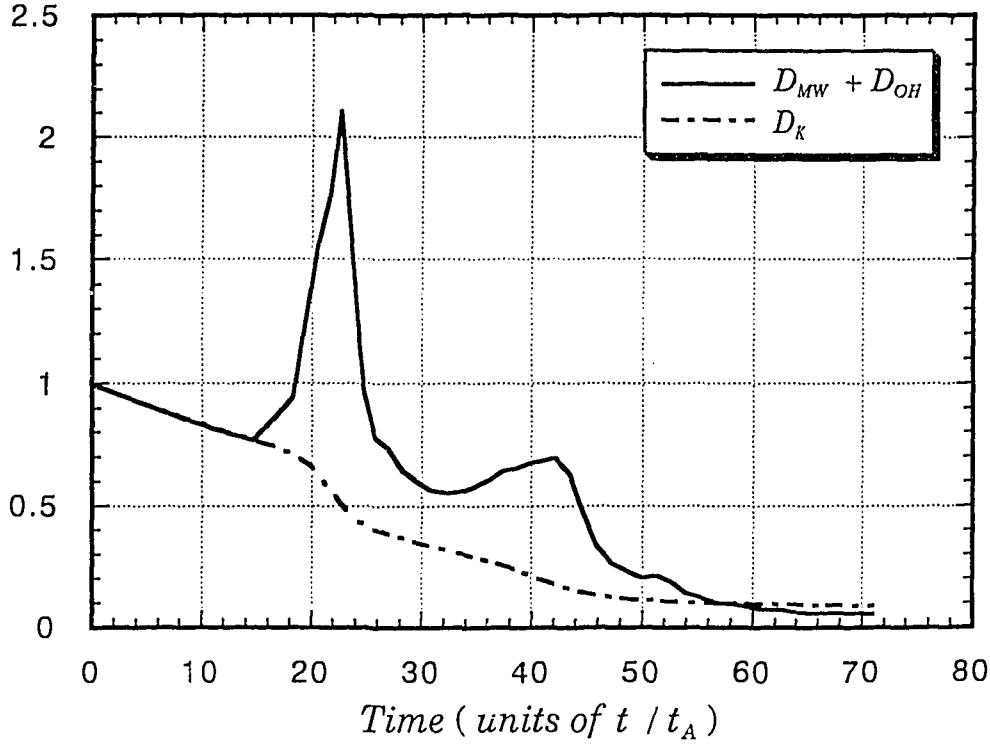
D_{MW} + D_{OH}
D_K
0
0.5
1
1.5
2
2.5
0
10
20
30
40
50
60
70
80
Time (units of t / t_A)

*Fig.*2

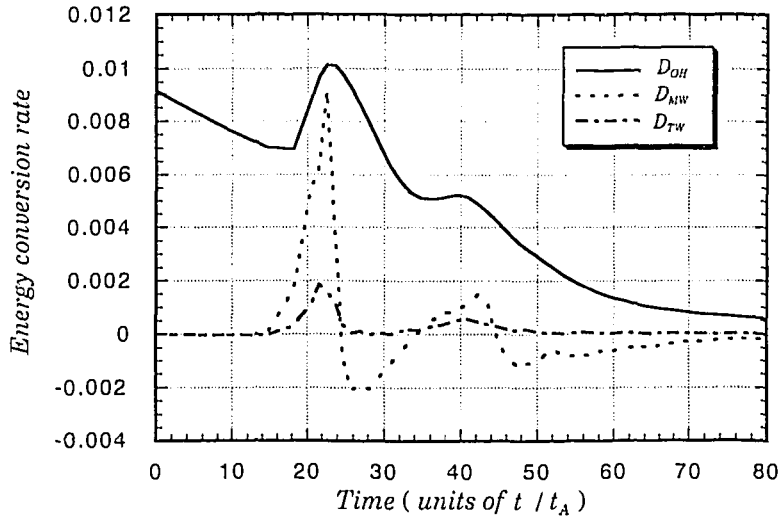

Fig.3

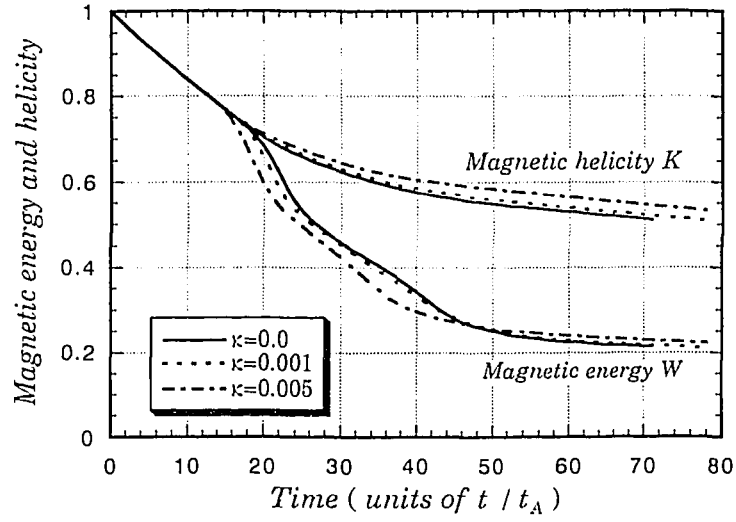

Fig.4

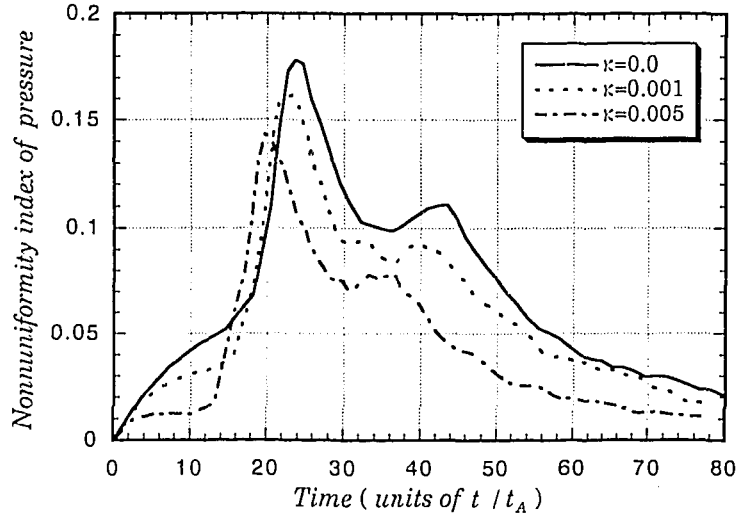

Fig.5

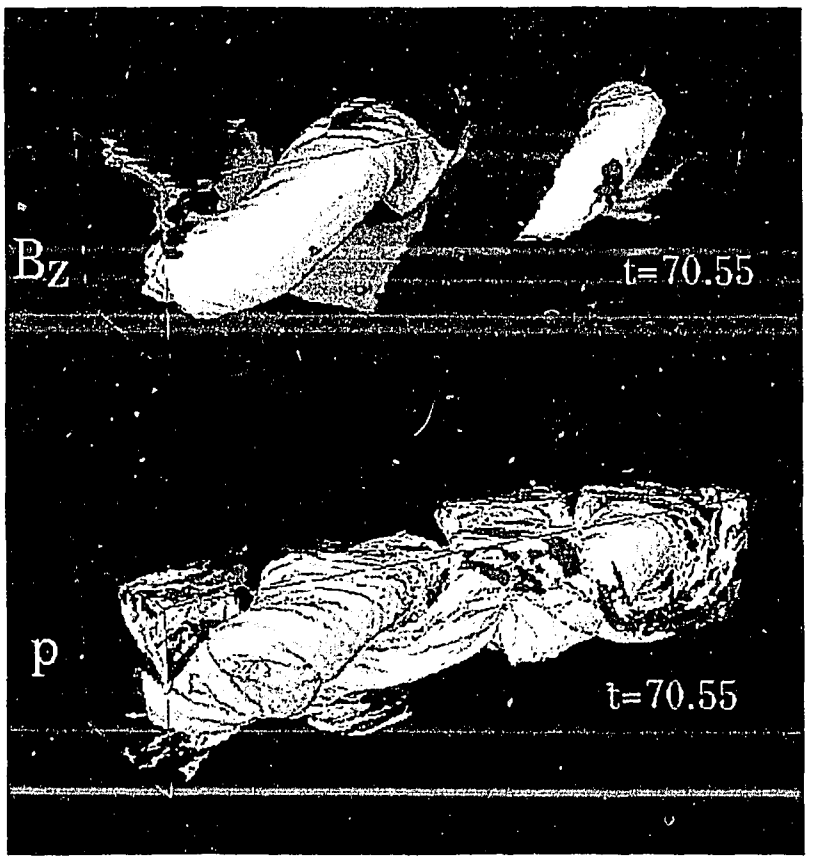

*Fig.*6

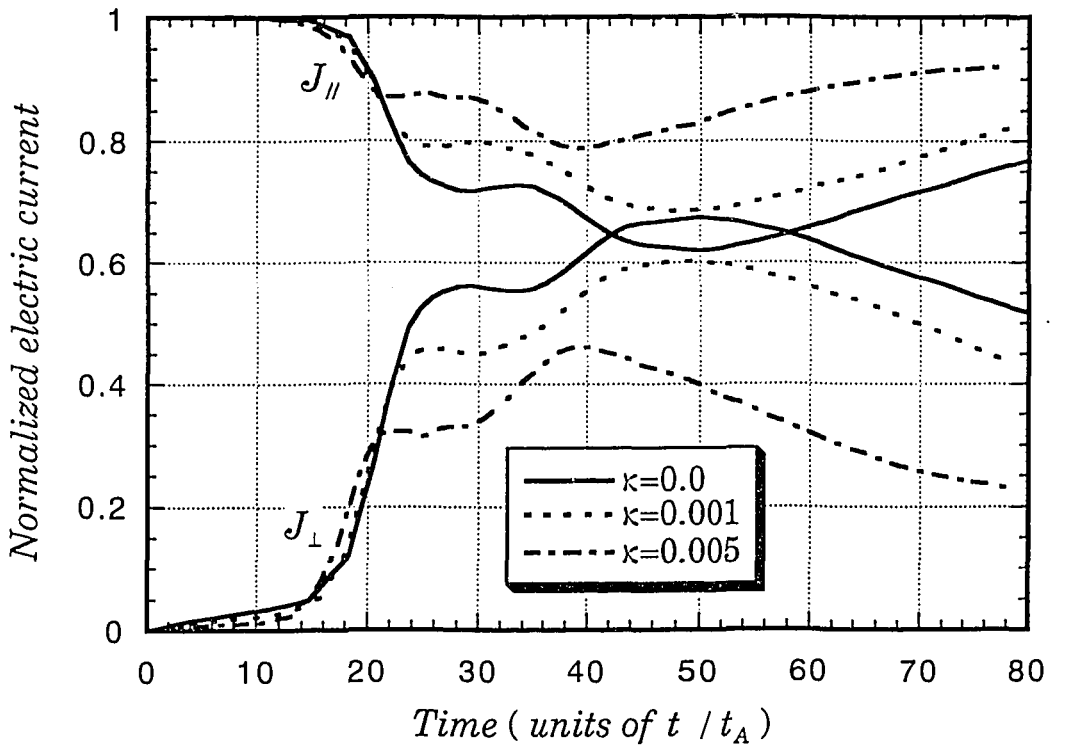
Normalized electric current
1
0.8
0.6
0.4
0.2
0
$J_{//}$
$J_{\perp}$
κ=0.0
κ=0.001
κ=0.005
0
10
20
30
40
50
60
70
80
Time (units of t / t_A)

Fig.7

Recent Issues of NIFS Series

NIFS-344 B.B.Kadomtsev, K. Itoh, S.-I. Itoh
Fast Change in Core Transport after L-H Transition; Mar. 1995

NIFS-345 W.X. Wang, M. Okamoto, N. Nakajima and S. Murakami,
An Accurate Nonlinear Monte Carlo Collision Operator; Mar. 1995

NIFS-346 S. Sasaki, S. Takamura, S. Masuzaki, S. Watanabe, T. Kato, K. Kadota,
Helium I Line Intensity Ratios in a Plasma for the Diagnostics of Fusion Edge Plasmas; Mar. 1995

NIFS-347 M. Osakabe,
Measurement of Neutron Energy on D-T Fusion Plasma Experiments; Apr. 1995

NIFS-348 M. Sita Janaki, M.R. Gupta and Brahmananda Dasgupta,
Adiabatic Electron Acceleration in a Cnoidal Wave; Apr. 1995

NIFS-349 J. Xu, K. Ida and J. Fujita,
A Note for Pitch Angle Measurement of Magnetic Field in a Toroidal Plasma Using Motional Stark Effect; Apr. 1995

NIFS-350 J. Uramoto,
Characteristics for Metal Plate Penetration of a Low Energy Negative Muonlike or Pionlike Particle Beam: Apr. 1995

NIFS-351 J. Uramoto,
An Estimation of Life Time for A Low Energy Negative Pionlike Particle Beam: Apr. 1995

NIFS-352 A. Taniike,
Energy Loss Mechanism of a Gold Ion Beam on a Tandem Acceleration System: May 1995

NIFS-353 A. Nishizawa, Y. Hamada, Y. Kawasumi and H. Iguchi,
Increase of Lifetime of Thallium Zeolite Ion Source for Single-Ended Accelerator: May 1995

NIFS-354 S. Murakami, N. Nakajima, S. Okamura and M. Okamoto,
Orbital Aspects of Reachable β Value in NBI Heated Heliotron/Torsatrons; May 1995

NIFS-355 H. Sugama and W. Horton,
Neoclassical and Anomalous Transport in Axisymmetric Toroidal Plasmas with Electrostatic Turbulence; May 1995

NIFS-356 N. Ohyabu
A New Boundary Control Scheme for Simultaneous Achievement

of H-mode and Radiative Cooling (SHC Boundary); May 1995

NIFS-357 Y. Hamada, K.N. Sato, H. Sakakita, A. Nishizawa, Y. Kawasumi, R. Liang, K. Kawahata, A. Ejiri, K. Toi, K. Narihara, K. Sato, T. Seki, H. Iguchi, A. Fujisawa, K. Adachi, S. Hidekuma, S. Hirokura, K. Ida, M. Kojima, J. Koong, R. Kumazawa, H. Kuramoto, T. Minami,. M. Sasao, T. Tsuzuki, J.Xu, I. Yamada, and T. Watari,
Large Potential Change Induced by Pellet Injection in JIPP T-IIU Tokamak Plasmas; May 1995

NIFS-358 M. Ida and T. Yabe,
Implicit CIP (Cubic-Interpolated Propagation) Method in One Dimension; May 1995

NIFS-359 A. Kageyama, T. Sato and The Complexity Simulation Group,
Computer Has Solved A Historical Puzzle: Generation of Earth's Dipole Field; June 1995

NIFS-360 K. Itoh, S.-I. Itoh, M. Yagi and A. Fukuyama,
Dynamic Structure in Self-Sustained Turbulence; June 1995

NIFS-361 K. Kamada, H. Kinoshita and H. Takahashi,
Anomalous Heat Evolution of Deuteron Implanted Al on Electron Bombardment; June 1995

NIFS-362 V.D. Pustovitov,
Suppression of Pfirsch-schlüter Current by Vertical Magnetic Field in Stellarators; June 1995

NIFS-363 A. Ida, H. Sanuki and J. Todoroki
An Extended K-dV Equation for Nonlinear Magnetosonic Wave in a Multi-Ion Plasma; June 1995

NIFS-364 H. Sugama and W. Horton
Entropy Production and Onsager Symmetry in Neoclassical Transport Processes of Toroidal Plasmas; July 1995

NIFS-365 K. Itoh, S.-I. Itoh, A. Fukuyama and M. Yagi,
On the Minimum Circulating Power of Steady State Tokamaks; July 1995

NIFS-366 K. Itoh and Sanae-I. Itoh,
The Role of Electric Field in Confinement; July 1995

NIFS-367 F. Xiao and T. Yabe,
A Rational Function Based Scheme for Solving Advection Equation; July 1995

NIFS-368 Y. Takeiri, O. Kaneko, Y. Oka, K. Tsumori, E. Asano, R. Akiyama, T. Kawamoto and T. Kuroda,

Multi-Beamlet Focusing of Intense Negative Ion Beams by Aperture Displacement Technique; Aug. 1995

NIFS-369 A. Ando, Y. Takeiri, O. Kaneko, Y. Oka, K. Tsumori, E. Asano, T. Kawamoto, R. Akiyama and T. Kuroda,
Experiments of an Intense H- Ion Beam Acceleration; Aug. 1995

NIFS-370 M. Sasao, A. Taniike, I. Nomura, M. Wada, H. Yamaoka and M. Sato,
Development of Diagnostic Beams for Alpha Particle Measurement on ITER; Aug. 1995

NIFS-371 S. Yamaguchi, J. Yamamoto and O. Motojima;
A New Cable -in conduit Conductor Magnet with Insulated Strands; Sep. 1995

NIFS-372 H. Miura,
Enstrophy Generation in a Shock-Dominated Turbulence; Sep. 1995

NIFS-373 M. Natsir, A. Sagara, K. Tsuzuki, B. Tsuchiya, Y. Hasegawa, O. Motojima,
Control of Discharge Conditions to Reduce Hydrogen Content in Low Z Films Produced with DC Glow; Sep. 1995

NIFS-374 K. Tsuzuki, M. Natsir, N. Inoue, A. Sagara, N. Noda, O. Motojima, T. Mochizuki, I. Fujita, T. Hino and T. Yamashina,
Behavior of Hydrogen Atoms in Boron Films during H_2 and He Glow Discharge and Thermal Desorption; Sep. 1995

NIFS-375 U. Stroth, M. Murakami, R.A. Dory, H. Yamada, S. Okamura, F. Sano and T. Obiki,
Energy Confinement Scaling from the International Stellarator Database; Sep. 1995

NIFS-376 S. Bazdenkov, T. Sato, K. Watanabe and The Complexity Simulation Group,
Multi-Scale Semi-Ideal Magnetohydrodynamics of a Tokamak Plasma; Sep. 1995

NIFS-377 J. Uramoto,
Extraction of Negative Pionlike Particles from a H2 or D2 Gas Discharge Plasma in Magnetic Field; Sep. 1995

NIFS-378 K. Akaishi,
Theoretical Consideration for the Outgassing Characteristics of an Unbaked Vacuum System; Oct. 1995

NIFS-379 H. Shimazu, S. Machida and M. Tanaka,
Macro-Particle Simulation of Collisionless Parallel Shocks; Oct. 1995

NIFS-380 N. Kondo and Y. Kondoh,
Eigenfunction Spectrum Analysis for Self-organization in Dissipative

Solitons; Oct. 1995

NIFS-381 Y. Kondoh, M. Yoshizawa, A. Nakano and T. Yabe,
Self-organization of Two-dimensional Incompressible Viscous Flow in a Friction-free Box; Oct. 1995

NIFS-382 Y.N. Nejoh and H. Sanuki,
The Effects of the Beam and Ion Temperatures on Ion-Acoustic Waves in an Electron Beam-Plasma System; Oct. 1995

NIFS-383 K. Ichiguchi, O. Motojima, K. Yamazaki, N. Nakajima and M. Okamoto
Flexibility of LHD Configuration with Multi-Layer Helical Coils; Nov. 1995

NIFS-384 D. Biskamp, E. Schwarz and J.F. Drake,
Two-dimensional Electron Magnetohydrodynamic Turbulence; Nov. 1995

NIFS-385 H. Kitabata, T. Hayashi, T. Sato and Complexity Simulation Group,
Impulsive Nature in Collisional Driven Reconnection; Nov. 1995

NIFS-386 Y. Katoh, T. Muroga, A. Kohyama, R.E. Stoller, C. Namba and O. Motojima,
Rate Theory Modeling of Defect Evolution under Cascade Damage Conditions:The Influence of Vacancy-type Cascade Remnants and Application to the Defect Production Chracterization by Microstructural Analysis; Nov. 1995

NIFS-387 K. Araki, S. Yanase and J. Mizushima,
Symmetry Breaking by Differential Rotation and Saddle-node Bifurcation of the Thermal Convection in a Spherical Shell; Dec. 1995

NIFS-388 V.D. Pustovitov,
Control of Pfirsch-Schlüter Current by External Poloidal Magnetic Field in Conventional Stellarators: Dec. 1995

NIFS-389 K. Akaishi,
On the Outgassing Rate Versus Time Characteristics in the Pump-down of an Unbaked Vacuum System; Dec. 1995

NIFS-390 K.N. Sato, S. Murakami, N. Nakajima, K. Itoh,
Possibility of Simulation Experiments for Fast Particle Physics in Large Helical Device (LHD); Dec. 1995

NIFS-391 W.X.Wang, M. Okamoto, N. Nakajima, S. Murakami and N. Ohyabu,
A Monte Carlo Simulation Model for the Steady-State Plasma in the Scrape-off Layer; Dec. 1995